Print-on-Demand Facsimile of Online Articles

PALAIOS

Emphasizing the Impact of Life on Earth's History

August 2022 Volume 37, No. 8

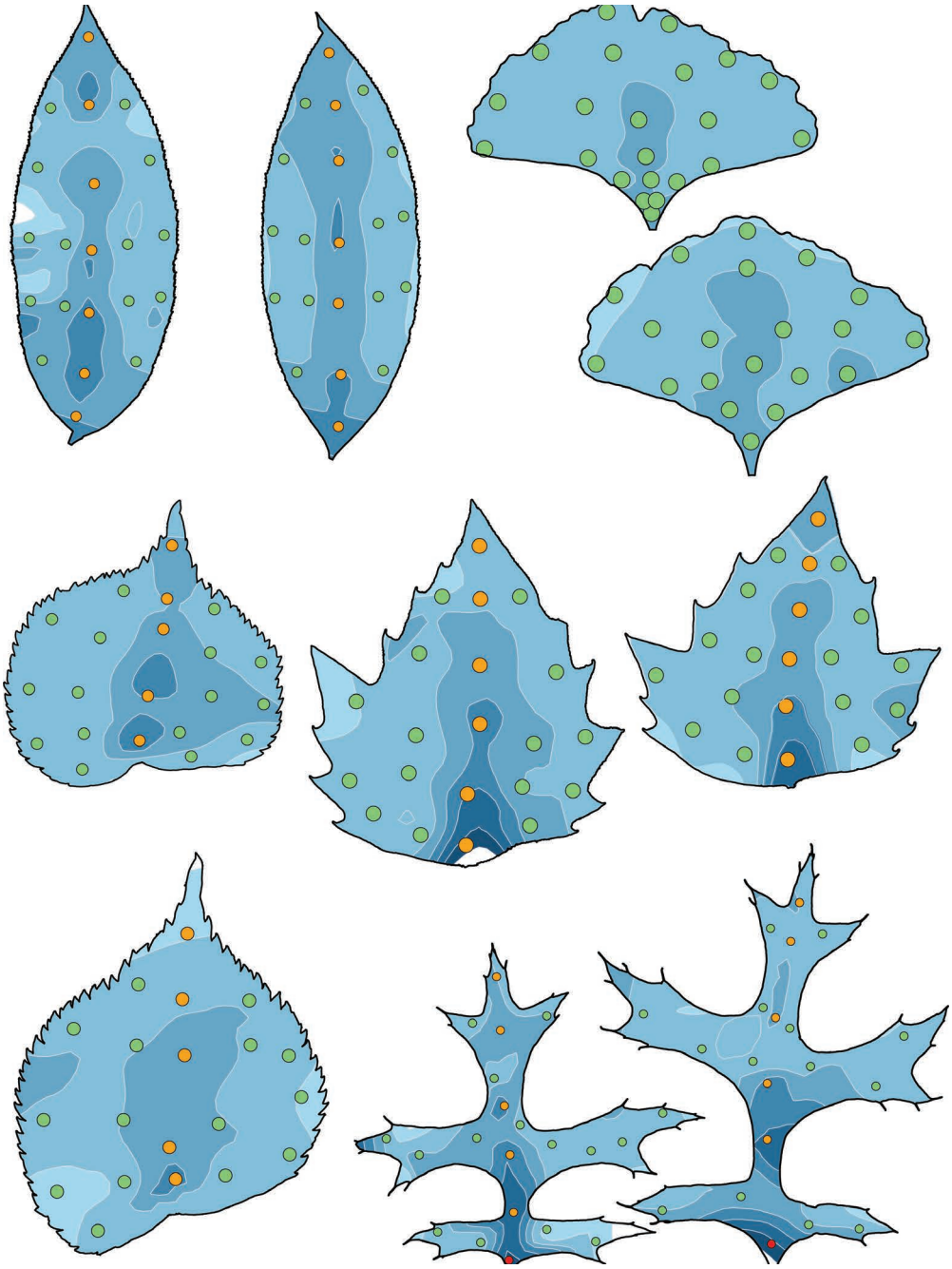

An International Journal of SEPM
(Society for Sedimentary Geology)

PALAIOS
Emphasizing the impact of life on Earth's history

PALAIOS, 2022, v. 37, 411–417
Research Article
DOI: http://dx.doi.org/10.2110/palo.2022.001

BULK CARBON ISOTOPIC VARIABILITY WITHIN LEAVES

DANA L. ROYER[1] AND MICHAEL T. HREN[2,3]
[1]Department of Earth and Environmental Sciences, Wesleyan University, Middletown, Connecticut 06459, USA
[2]Department of Earth Sciences, University of Connecticut, Storrs, Connecticut 06269, USA
[3]Department of Chemistry, University of Connecticut, Storrs, Connecticut 06269, USA
email:droyer@wesleyan.edu

ABSTRACT: **The stable carbon isotopic composition ($\delta^{13}C$) of fossil leaves is a simple and common measurement that provides information about paleophysiology, paleoecology, and paleoclimate. Variance in $\delta^{13}C$ is typically assessed across leaves; comparatively little is known about variance within leaves, a potential source of unquantified uncertainty. Here we systematically analyze the spatial patterns of bulk $\delta^{13}C$ in fresh leaves of 10 tree species (two leaves per species; 21 or 22 analyses per leaf). We find that samples containing midvein tissue are markedly higher in $\delta^{13}C$ than non-midvein tissue from the same leaf (median = +0.85‰), with samples containing only midvein tissue offset by as much as +3.01‰. The non-midvein samples are less variable—the typical range within a single leaf is <1‰—and do not show any consistent spatial patterns. In cases where whole fossil leaves cannot be analyzed, we recommend sampling as many randomized areas without major veins as is feasible.**

INTRODUCTION

Fossil plants provide key information for reconstructing terrestrial climate and ecology (McElwain 2018). Their stable carbon isotopic composition ($\delta^{13}C$), for example, is sensitive to: (1) the $\delta^{13}C$ of the carbon source, which is almost always atmospheric CO_2 and (2) the balance between the input of CO_2 to the leaf (controlled in part by leaf conductance and respiratory processes) and the assimilation of CO_2 into leaf carbon (Farquhar et al. 1989). Owing to these sensitivities, the $\delta^{13}C$ of fossil plant carbon has been used to interpret patterns in atmospheric $\delta^{13}C$ (Nordt et al. 2016), canopy openness (Graham et al. 2019), salt stress (Nguyen Tu et al. 1999), moisture balance (Schlanser et al. 2020), photosynthetic pathway (C_3 vs. C_4) (Polissar et al. 2019), and atmospheric CO_2 concentration (Cui et al. 2020). Leaf $\delta^{13}C$ is also a key input for leaf gas-exchange proxies for atmospheric CO_2 concentration (Konrad et al. 2008, 2017; Franks et al. 2014). The measurement of fossil plant $\delta^{13}C$ has become routine and very common (e.g., see compilation in Nordt et al. 2016).

The confidence in interpreting environmental information from plant $\delta^{13}C$ is strongly constrained by the variance in the isotopic signal. When measuring fossil leaf $\delta^{13}C$, this variability is generally assessed across leaves (e.g., Maxbauer et al. 2014). In contrast, less is known about the variability of bulk $\delta^{13}C$ within leaves, even in living plants. This means that the true $\delta^{13}C$ uncertainty in a set of measured fossil leaves is probably being underestimated. The specter of intra-leaf variability is especially problematic for fossil studies because fossil leaves are usually fragmented.

In living plants, leaf-vein tissue has a higher $\delta^{13}C$ than non-vein tissue: in the nine species reported by Schleser (1990), Spain and Feuvre (1997), and Badeck et al. (2009), this difference ranges from +0.8 to +1.9‰. Different leaf components have characteristic $\delta^{13}C$ values. In particular, sugar, starch, protein, and cellulose usually have a higher $\delta^{13}C$ than lipids and lignin (Badeck et al. 2005; Bowling et al. 2008). Thus, the high proportion of cellulose in vein tissue could explain the tissue difference in $\delta^{13}C$. Schleser (1990), however, finds a similar vein versus non-vein isotopic offset in the cellulose fraction, casting doubt on this explanation. Badeck et al. (2009) instead argue that post-photosynthetic metabolism—which is more common in photosynthetic tissue than in vein (non-photosynthetic) tissue—can explain the offset because secondary metabolites usually have a lower $\delta^{13}C$ (see also Cernusak et al. 2009).

A few studies report $\delta^{13}C$ patterns within leaves excluding first-order (e.g., midvein) and second-order veins (*sensu* Ellis et al. 2009), with no clear trend emerging. Schleser (1990) finds no spatial patterns and minimal variance (max–min = 0.3‰) in *Fagus sylvatica* (European beech). Along similar lines, three conifer genera with needle-like leaves, both living and fossil, show a limited intra-leaf $\delta^{13}C$ range (<1‰) and no spatial patterns (Liang et al. 2022). In contrast, Farquhar and Gan (2003) observe a base-to-tip gradient of -0.6‰ in *Gossypium hirsutum* (cotton); Spangenberg et al. (2021) report a similar gradient for two grape cultivars. Stomatal (Farquhar and Gan 2003; Affek et al. 2006; Nardini et al. 2008) and mesophyll (Kodama et al. 2011) conductance is often highest towards the leaf tip, but not always (Li et al. 2013). Because a high conductance facilitates a high flux of CO_2 into the leaf, this can lead to a larger carbon isotopic fractionation during photosynthesis (Ehleringer 1990), and thus explain a negative base-to-tip $\delta^{13}C$ gradient.

Other studies report a base-to-tip gradient of 0 to -3‰ in seven living and three fossil species, but their sampling designs either explicitly include second-order (Grein et al. 2010) and/or first-order (Gao et al. 2015) veins, or are not adequately described (Chakraborty et al. 2011). As such, any isotopic gradients in these studies may be driven by varying proportions of vein tissue, especially considering that first- and second-order vein density is often highest towards the leaf base (e.g., leaves with a palmate vein architecture).

Together, these data point to an intra-leaf variability—typically < 1.5‰—that is similar to or smaller than the range across leaves in a single tree (e.g., Graham et al. 2014). The ^{12}C enrichment in veins may explain much of this variability. Depending on the fossil application, this uncertainty could be important to take into account: in leaf gas-exchange proxies for atmospheric CO_2, for example, a difference of 1‰ in leaf $\delta^{13}C$ can shift the estimated CO_2 concentration by 10–20% (Maxbauer et al. 2014).

Published Online: August 2022
 0883-1351/22/037-411

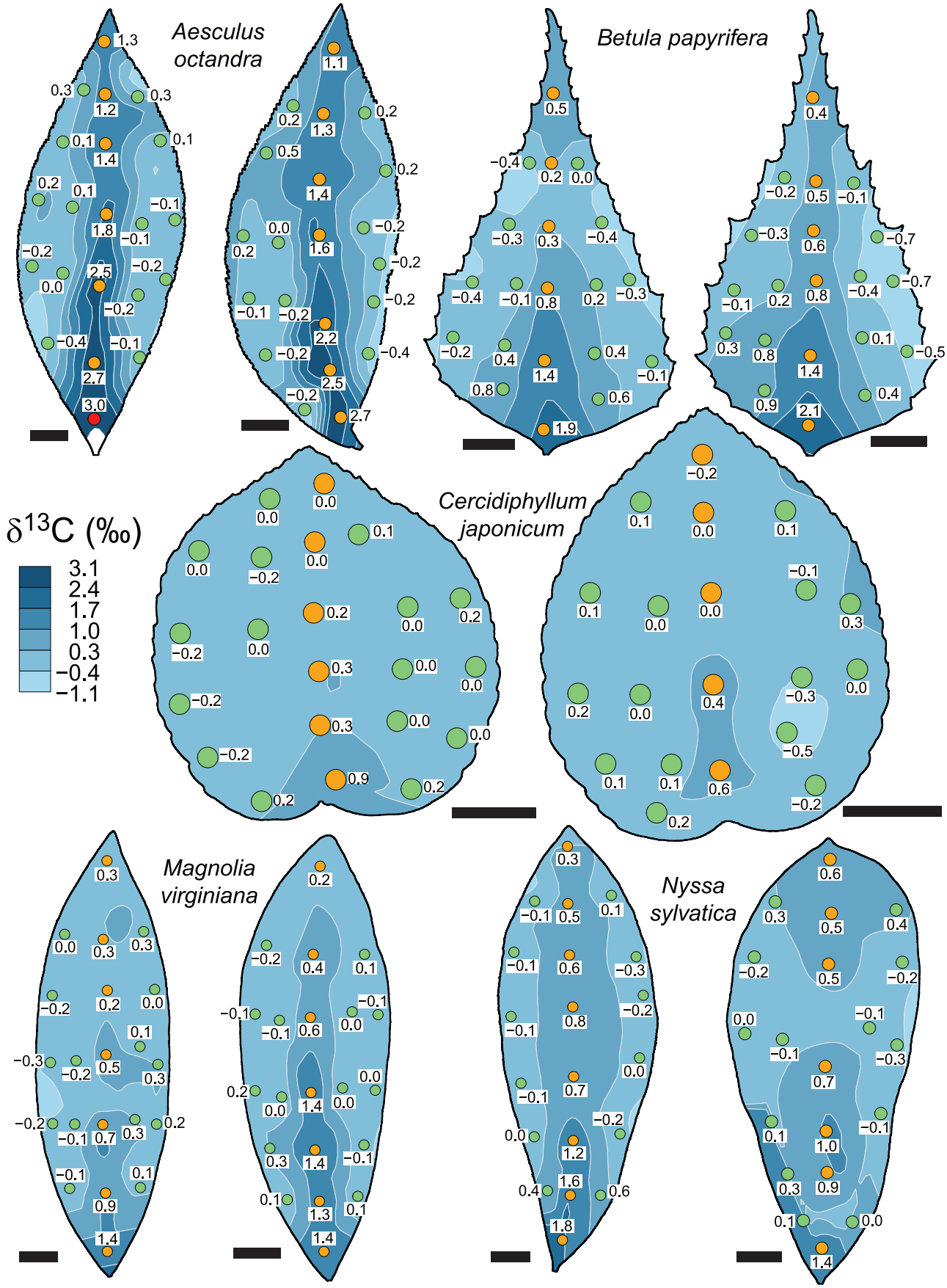

FIG. 1.—$\delta^{13}C$ maps for five species. For each leaf, isotopic values are expressed relative to the mean of samples that contain no midvein tissue (green symbols). Orange symbols = samples that include midvein tissue; red symbols = samples comprised only of midvein tissue; this color coding is identical across all figures. Scale bars = 1 cm. Sizes of circles roughly scale with the actual sizes of the leaf disks.

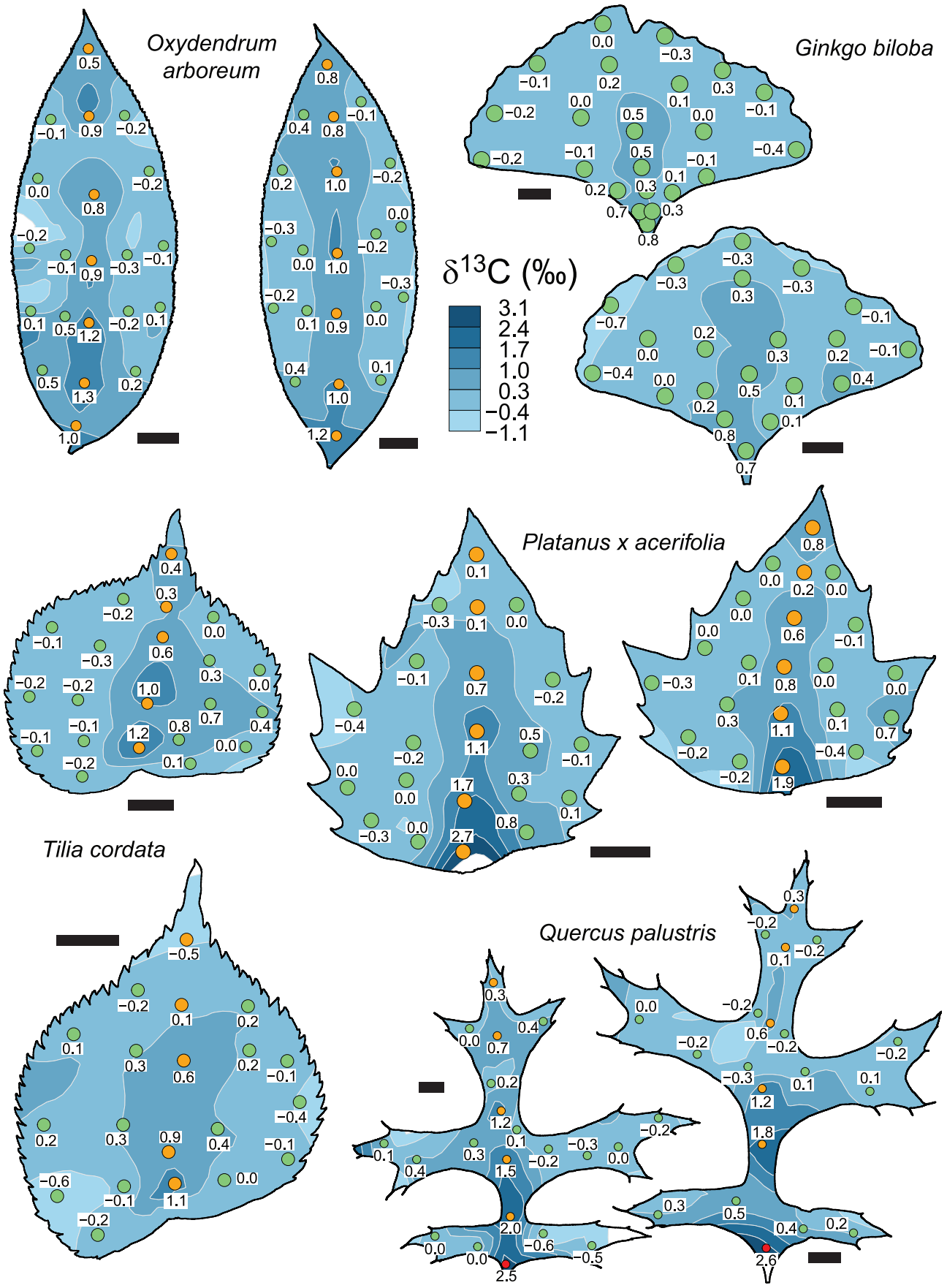

FIG. 2.—$\delta^{13}C$ maps for five species. For each leaf, isotopic values are expressed relative to the mean of samples that contain no midvein tissue (green symbols). For ginkgo, which lacks a midvein, the mean is based on all but the three or four basal-most samples, which have the highest density of vein tissue. Orange symbols = samples that include midvein tissue; red symbols = samples comprised only of midvein tissue; this color coding is identical across all figures. Scale bars = 1 cm. Sizes of circles roughly scale with the actual sizes of the leaf disks.

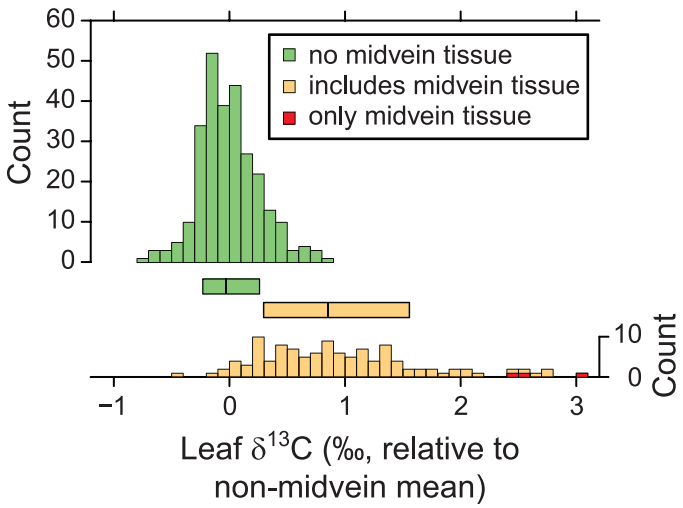

FIG. 3.—Distribution of relative $\delta^{13}C$ values. For the two horizontal bars in the middle, the vertical lines represent the medians and the widths of the bars span the 68th percentile ranges; the yellow bar includes the three midvein-only samples.

Most previous work has not explicitly mapped sampling locations with their associated $\delta^{13}C$, which blunts the ability to resolve spatial patterns. To address this limitation, here we map the intra-leaf distribution of $\delta^{13}C$ in nine angiosperm tree species and one broad-leaf gymnosperm (*Ginkgo biloba*) and then analyze these distributions in a spatially explicit manner. Our primary goals are to: (1) quantify how much $\delta^{13}C$ varies within leaves and (2) partition this variability between midvein and non-midvein tissue.

MATERIALS AND METHODS

We collected sun leaves from southern exposures of single trees from 10 species ~ 2 m off the ground in late June and early July 2021. The 10 species span nine different plant orders. All trees are on the campus of Wesleyan University, Middletown, Connecticut. Within an hour of sampling, leaves were dried in a plant press at 50°C for several days. For two leaves per species, we used a hole punch with a 3 mm diameter to remove 21 or 22 disks of material. Within each leaf, a subset of disks come from the midvein region, sampled from base to tip; all other disks avoid first-order veins (e.g., midvein) and mostly avoid second-order veins. The one exception is *Ginkgo biloba*, whose leaves contain a fan of equally sized veins; here we sampled systematically across the leaves, with disks near the leaf base and center containing the highest proportion of vein tissue.

Disks were loaded and balled into tin capsules (5 × 9 mm). For some of the heavier disks, only a subsample was used; sample masses ranged from 0.219 to 1.347 mg. For each disk, dry mass per area was calculated based on the mass of the full disk and an area assuming a circle with a 3 mm diameter.

The stable carbon isotopic compositions and total mass fractions of carbon and nitrogen were measured via high temperature combustion in a Costech Elemental Analyzer attached to a Thermo MAT 253 Plus IRMS using He as a carrier gas. The isotopic composition of unknown leaf samples were corrected for size and scale compression effects and drift using a suite of international reference materials that span the range of carbon isotopic variability and sample intensities. Reproducibility of standards over a range of sample sizes and throughout the duration of the run was < 0.1‰ 1σ. We also ran 18 replicate analyses, each based on two side-by-side leaf disks, cut in half and mixed; these paired measurements differed by up to 0.21‰ (mean = 0.07 ± 0.05‰ 1σ), which is similar to instrument error. See Online Supplemental File Table S1 for all isotopic data.

TABLE 1.—*$\delta^{13}C$ range within individual leaves for non-midvein samples.*

	$\delta^{13}C$ range (‰)	
Species (common name)	Leaf 1	Leaf 2
Aesculus octandra (yellow buckeye)	0.68	0.97
Betula papyrifera (paper birch)	1.17	1.63
Cercidiphyllum japonicum (katsura)	0.43	0.87
Ginkgo biloba (ginkgo)	1.15	1.46
Magnolia virginiana (sweet bay)	0.60	0.49
Nyssa sylvatica (black tupelo)	0.91	0.66
Oxydendrum arboreum (sourwood)	0.81	0.76
Platanus × *acerifolia* (London plane)	1.21	1.04
Quercus palustris (pin oak)	1.07	0.82
Tilia cordata (littleleaf linden)	1.01	1.01

For each leaf, we express $\delta^{13}C$ relative to the leaf-mean of disks that do not include midvein tissue; this normalization aids in seeing spatial patterns both within and across leaves. To map the isotopic data of a single leaf, we used ImageJ (https://imagej.nih.gov/ij/) to extract x-y coordinates of the leaf outline, scale bar, and center points of the disks; see Online Supplemental Data File 1 for instructions and example files. Next, in R (R Core Team 2021), we used the INTERP function in the AKIMA package (Akima and Gebhardt 2021) to interpret a grid of isotopic data from the measured data, followed by the ISOPOLY function in the SPATIALPOSITION package (Giraud and Commenges 2021) to create contours from the interpreted grid. We then plotted the contours, clipped to the coordinates of the leaf outline. See Online Supplemental Data File 1 for R code and an example input file.

RESULTS

Leaf disks with midvein tissue (orange and red symbols in Figs. 1, 2) have distinctly higher $\delta^{13}C$ values than disks without midvein tissue (blue symbols in Figs. 1, 2; see also Online Supplemental File Figs. S1, S2 for photographs of leaves with isotope values and no contours). For midvein samples, the median isotopic offset to the disk's leaf-mean of non-midvein $\delta^{13}C$ is +0.85‰, with an inner 68th percentile range of +0.30 to +1.56 ‰ (Fig. 3); there is a strong tail to high values (max = +3.01‰), with most of the highest values coming from disks comprised completely of vein tissue (red bars in Fig. 3). This contrasts with leaf disks containing no midvein tissue, which (by definition) have a mean isotopic offset of 0 ‰, and an inner 68th percentile range of -0.23 to +0.26‰. The difference between these two populations is statistically significant ($P = 2.2 \times 10^{-16}$; Wilcoxon rank sum test).

Within each leaf, the $\delta^{13}C$ of disks with midvein tissue declines from base to tip; this gradient across our 20 leaves varies from -0.4 to -2.6‰ (mean = -1.3‰; Figs. 1, 2). In contrast, disks without midvein tissue do not show consistent spatial patterns across species. In *Aesculus octandra*, tissue near the tip is ~ 0.5‰ higher than near the base, while in *Betula papyrifera* the reverse is true, with areas near the tip being > 0.5‰ lower than near the base (Fig. 1; see also Online Supplemental File Figs. S3, S4 for isotope maps that exclude midvein samples). In *Ginkgo biloba* and *Tilia cordata*, areas near the leaf center tend to have higher $\delta^{13}C$ values than areas near the margin (Fig. 2). In the other six species, no clear spatial patterns emerge (Figs. 1, 2). The within-leaf isotopic range for non-midvein tissue is relatively small, varying from 0.43‰ (*Cercidiphyllum japonicum*) to 1.63‰ (*B. papyrifera*), with a mean of 0.94‰ (Table 1).

Within individual leaves, mass per area often correlates significantly with $\delta^{13}C$ (Fig. 4): that is, areas of the leaf that are thicker or denser tend to

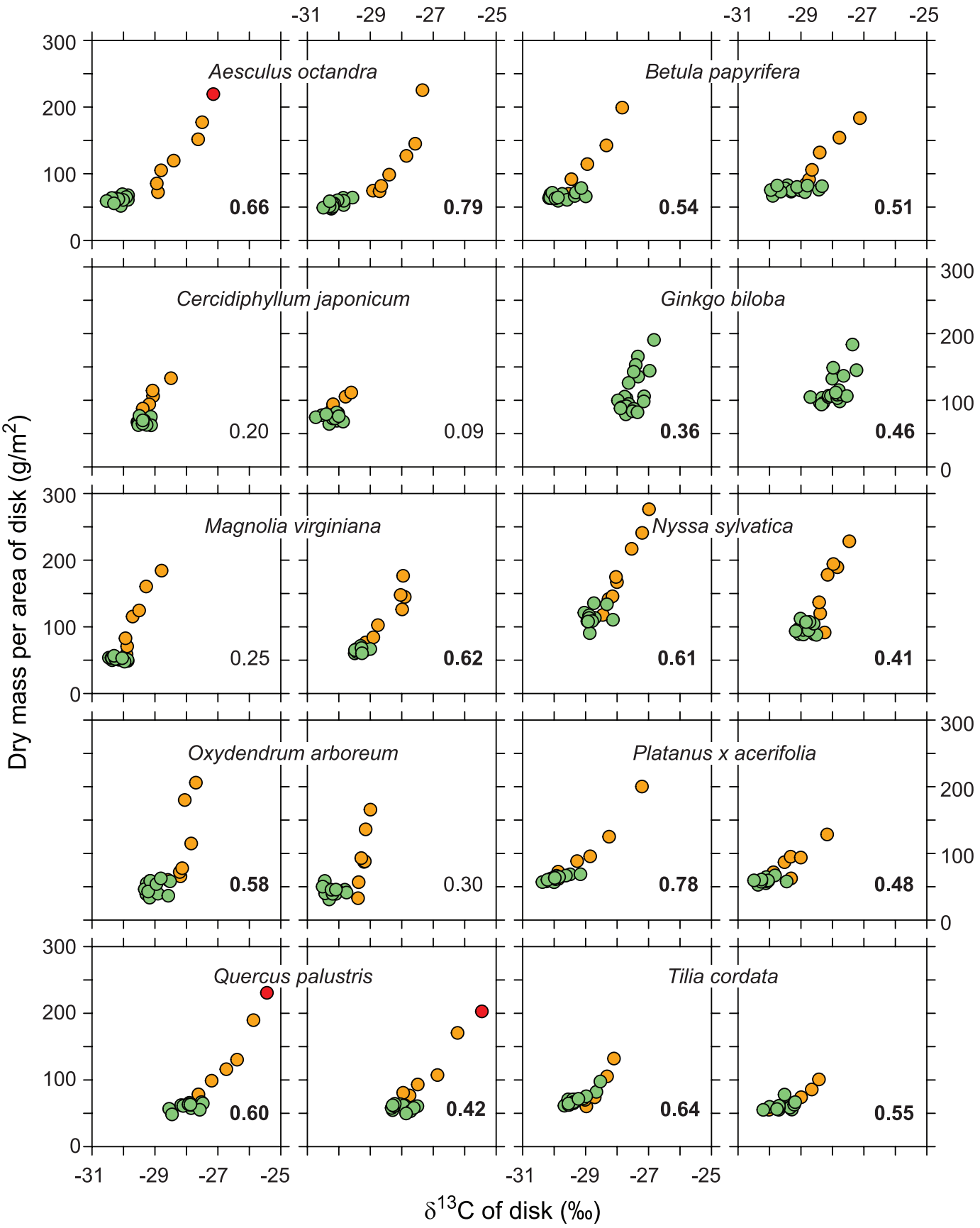

FIG. 4.—Correlations between leaf $\delta^{13}C$ and leaf dry mass per area in the sampled disks. Each panel summarizes a single leaf. Green symbols = samples lacking midvein tissue; orange symbols = samples with midvein tissue; red symbols = samples comprised only of midvein tissue; this color coding is identical across all figures. Numbers inside panels are Kendall's coefficient of rank correlation; values in bold have an associated $P < 0.05$.

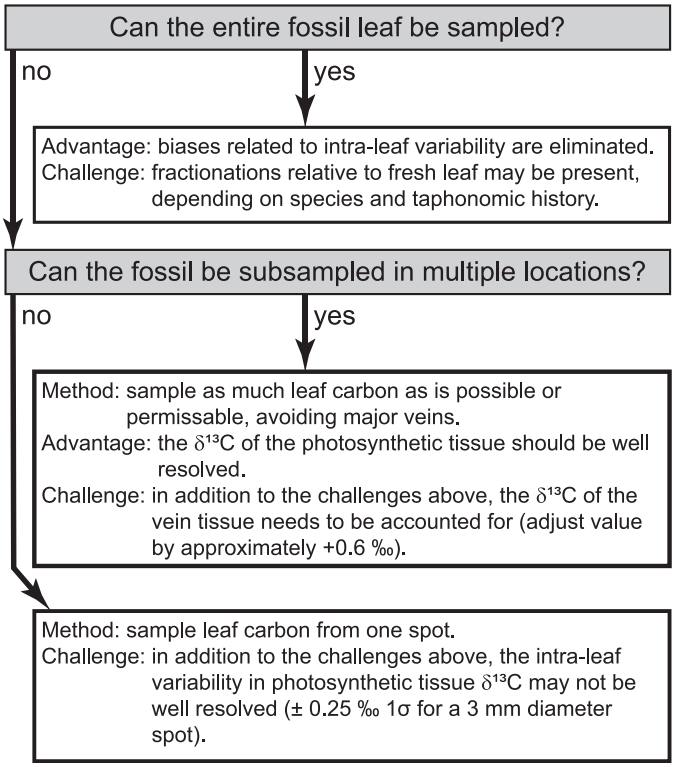

FIG. 5.—Decision tree for sampling fossil leaves.

have a higher $\delta^{13}C$. The same pattern holds for the C/N ratio (Online Supplemental File Fig. S5): proportionally carbon-rich areas of the leaf correlate with higher $\delta^{13}C$. In most of the leaves, the strength of these correlations is largely driven by the samples containing midvein tissue (orange and red symbols in Fig. 4 and Online Supplemental File Fig. S5). In some species, for example *Platanus* × *acerifolia* and *T. cordata*, the non-midvein areas also show the covariation, albeit weakly.

DISCUSSION

The $\delta^{13}C$ of samples containing midvein tissue is sharply higher than samples without midvein tissue (Figs. 1–4), with a mean within-leaf difference of 0.85‰. The sign of this offset is consistent with previous work (see Introduction) but demonstrated here for 10 additional species. We note that the three samples comprised entirely of midvein tissue, which come from the leaf-base region where the midvein is thickest, have very large positive offsets: 2.48, 2.60, and 3.01‰ (see red symbols in Figs. 1–4). These isotopic differences are considerably larger than previous reports (0.8 to 1.9‰; Schleser 1990; Spain and Le Feuvre 1997; Badeck et al. 2009).

Our midvein samples systematically decline in $\delta^{13}C$ from base to tip, with an average drop of -1.3‰ (Figs. 1, 2). This gradient is likely due to two factors. First, the midvein tissue itself may decline in $\delta^{13}C$ along its length. Indeed, Schleser (1990) reports a -1.2‰ base-to-tip drop in midvein-only tissue for a single *Fagus sylvatica* leaf. Second, our leaf disks from base to tip contain proportionally less midvein tissue, owing to midvein taper. This alone can explain the negative $\delta^{13}C$ gradient because non-midvein tissue has a lower $\delta^{13}C$ (Badeck et al. 2009; Cernusak et al. 2009). The strong correlation within leaves between $\delta^{13}C$ and both mass per area (Fig. 4) and C/N (Online Supplemental File Fig. S5) supports this second scenario because midveins, which are normally thick and non-photosynthetic, have a high mass per area and C/N relative to the rest of the leaf.

When excluding midvein samples, $\delta^{13}C$ varied on average by $\sim$ 1‰ within individual leaves (Table 1). This relatively small intra-leaf variability is in keeping with most previous observations (see Introduction). We find no consistent spatial pattern in this variability, also in keeping with previous work. And, in fact, the negative $\delta^{13}C$ gradient between samples near the leaf center versus margin observed in two species (*T. cordata* and *G. biloba*; Fig. 2) can be explained by correlated changes in vein tissue amount. In the case of ginkgo, with its fan-shaped architecture of first-order veins, vein density is highest near the leaf base and center, and lowest along the leaf margin. In the case of *Tilia*, the isotope gradient is largely driven by a few disks that contain second-order vein tissue, which have correspondingly high $\delta^{13}C$ (see also Online Supplemental File Fig. S2); these samples also underpin the (weak) correlation between $\delta^{13}C$ and mass per area in non-midvein samples (green circles in Fig. 4).

RECOMMENDATIONS FOR SAMPLING FOSSIL LEAVES

If our results are representative of plants more generally, they provide at least three insights about sampling fossil leaves for $\delta^{13}C$ (see Fig. 5 for summary). First, whole leaves should be analyzed whenever possible, thereby avoiding any biasing due to natural within-leaf variability. Please note, however, that preferential degradation of more labile tissue in leaves during the burial process can lead to isotopic fractionation. For example, photosynthetic tissue may decay more quickly than recalcitrant vein tissue, causing a shift to higher $\delta^{13}C$ values, even if the whole leaf is sampled. Cuticle also tends to preferentially preserve and can be isotopically offset from the bulk whole-leaf: Royer and Hren (2017) report across 175 species a $\pm$ 1‰ 1σ range in this offset.

Second, if whole-leaf analysis is not possible, avoiding first- and second-order veins is best, because veins have a distinctly high $\delta^{13}C$. If the goal in measuring $\delta^{13}C$ is to estimate whole-leaf $\delta^{13}C$, avoiding major veins will yield more precise and probably more accurate estimates. For example, if a leaf is sampled twice, once near the leaf base with a high proportion of vein tissue and once mid-lamina with no large veins, the mean $\delta^{13}C$ will likely be higher than the whole-leaf $\delta^{13}C$ (i.e., not accurate) and the estimated variance will be higher than a random set of samples from the same leaf (i.e., not precise). We note, however, that avoiding major veins will result in a mean $\delta^{13}C$ that is lower than the whole-leaf $\delta^{13}C$. We estimate that first- and second-order veins constitute $\approx$ 24% of the total leaf mass, assuming these veins comprise $\sim$ 6% of the projected leaf area (Sack et al. 2012) but $\sim$ 4× the mass per area (compare red vs. blue symbols in Fig. 4). If we also assume that first- and second-order vein tissue is + 2.5‰ relative to tissue excluding these veins (which may be on the high side: Schleser 1990; Spain and Le Feuvre 1997; Badeck et al. 2009), sampling that excludes these veins may lead to a mean $\delta^{13}C$ that is $\approx$ 0.6‰ lower than the true leaf mean.

Third, sampling an individual leaf in multiple places is best because small single samples of non-midvein tissue can deviate from the leaf mean by as much as 1‰ (Figs. 1, 2, Table 1). If only one sample is possible, we recommend adding a $\pm$ 0.25‰ 1σ uncertainty, which corresponds closely to the 68% percentile range of all non-midvein samples in our data set (green horizontal bar in Fig. 3). Because most species do not appear to have strong spatial patterns in non-midvein $\delta^{13}C$, sampling location is not critical.

SUPPLEMENTAL MATERIAL

Data are available from the PALAIOS Data Archive: https://www.sepm.org/supplemental-materials.

REFERENCES

Affek, H.P., Krisch, M.J., and Yakir, D., 2006, Effects of intraleaf variations in carbonic anhydrase activity and gas exchange on leaf $C^{18}OO$ isoflux in *Zea mays*: New Phytologist, v. 169, p. 321–329, doi: 10.1111/j.1469-8137.2005.01603.x.

Akima, H. and Gebhardt, A., 2021, akima: Interpolation of irregularly and regularly spaced data: R package version 0.6-2.1, https://CRAN.R-project.org/package=akima.

Badeck, F.-W., Fontaine, J.-L., Dumas, F., and Ghashghaie, J., 2009, Consistent patterns in leaf lamina and leaf vein carbon isotope composition across ten herbs and tree species: Rapid Communications in Mass Spectrometry, v. 23, p. 2455–2460, doi: 10.1002/rcm.4054.

Badeck, F.-W., Tcherkez, G., Nogués, S., Piel, C., and Ghashghaie, J., 2005, Post-photosynthetic fractionation of stable carbon isotopes between plant organs—a widespread phenomenon: Rapid Communications in Mass Spectrometry, v. 19, p. 1381–1391, doi: 10.1002/rcm.1912.

Bowling, D.R., Pataki, D.E., and Randerson, J.T., 2008, Carbon isotopes in terrestrial ecosystem pools and CO_2 fluxes: New Phytologist, v. 178, p. 24–40, doi: 10.1111/j.1469-8137.2007.02342.x.

Cernusak, L.A., Tcherkez, G., Keitel, C., Cornwell, W.K., Santiago, L.S., Knohl, A., Barbour, M.M., Williams, D.G., Reich, P.B., Ellsworth, D.S., Dawson, T.E., Griffiths, H.G., Farquhar, G.D., and Wright, I.J., 2009, Why are non-photosynthetic tissues generally ^{13}C enriched compared with leaves in C_3 plants? Review and synthesis of current hypotheses: Functional Plant Biology, v. 36, p. 199–213, doi: 10.1071/FP08216.

Chakraborty, S., Jana, B.N., Bhattacharya, S.K., and Robertson, I., 2011, Carbon isotopic composition of fossil leaves from the Early Cretaceous sediments of western India: Journal of Earth System Science, v. 120, p. 703–711, doi: 10.1007/s12040-011-0098-x.

Cui, Y., Schubert, B.A., and Jahren, A.H., 2020, A 23 m.y. record of low atmospheric CO_2: Geology, v. 48, p. 888–892, doi: 10.1130/g47681.1.

Ehleringer, J.R., 1990, Correlations between carbon isotope discrimination and leaf conductance to water vapor in common beans: Plant Physiology, v. 93, p. 1422–1425, doi: 10.1104/pp.93.4.1422.

Ellis, B., Daly, D.C., Hickey, L.J., Johnson, K.R., Mitchell, J.D., Wilf, P., and Wing, S.L., 2009, Manual of Leaf Architecture: Cornell University Press, Ithaca, 190 p.

Farquhar, G.D., Ehleringer, J.R., and Hubick, K.T., 1989, Carbon isotope discrimination and photosynthesis: Annual Review of Plant Physiology and Plant Molecular Biology, v. 40, p. 503–537, doi: 10.1146/annurev.pp.40.060189.002443.

Farquhar, G.D. and Gan, K.S., 2003, On the progressive enrichment of the oxygen isotopic composition of water along a leaf: Plant, Cell and Environment, v. 26, p. 801–819, doi: 10.1046/j.1365-3040.2003.01013.x.

Franks, P.J., Royer, D.L., Beerling, D.J., Van de Water, P.K., Cantrill, D.J., Barbour, M.M., and Berry, J.A., 2014, New constraints on atmospheric CO_2 concentration for the Phanerozoic: Geophysical Research Letters, v. 41, p. 4685–4694, doi: 10.1002/2014gl060457.

Gao, L., Guimond, J., Thomas, E., and Huang, Y., 2015, Major trends in leaf wax abundance, δ^2H and $\delta^{13}C$ values along leaf venation in five species of C_3 plants: physiological and geochemical implications: Organic Geochemistry, v. 78, p. 144–152, doi: 10.1016/j.orggeochem.2014.11.005.

Giraud, T. and Commenges, H., 2021, SpatialPosition: spatial position models: R package version 2.1.1., https://CRAN.R-project.org/package=SpatialPosition.

Graham, H.V., Herrera, F., Jaramillo, C., Wing, S.L., and Freeman, K.H., 2019, Canopy structure in Late Cretaceous and Paleocene forests as reconstructed from carbon isotope analyses of fossil leaves: Geology, v. 47, p. 977–981, doi: 10.1130/g46152.1.

Graham, H.V., Patzkowsky, M.E., Wing, S.L., Parker, G.G., Fogel, M.L., and Freeman, K.H., 2014, Isotopic characteristics of canopies in simulated leaf assemblages: Geochimica et Cosmochimica Acta, v. 144, p. 82–95, doi: 10.1016/j.gca.2014.08.032.

Grein, M., Roth-Nebelsick, A., and Wilde, V., 2010, Carbon isotope composition of middle Eocene leaves from the Messel Pit, Germany: Palaeodiversity, v. 3, p. 1–7.

Kodama, N., Cousins, A., Tu, K.P., and Barbour, M.M., 2011, Spatial variation in photosynthetic CO_2 carbon and oxygen isotope discrimination along leaves of the monocot triticale (*Triticum* × *Secale*) relates to mesophyll conductance and the Péclet effect: Plant, Cell and Environment, v. 34, p. 1548–1562, doi: 10.1111/j.1365-3040.2011.02352.x.

Konrad, W., Katul, G., Roth-Nebelsick, A., and Grein, M., 2017, A reduced order model to analytically infer atmospheric CO_2 concentration from stomatal and climate data: Advances in Water Resources, v. 104, p. 145–157, doi: 10.1016/j.advwatres.2017.03.018.

Konrad, W., Roth-Nebelsick, A., and Grein, M., 2008, Modelling of stomatal density response to atmospheric CO_2: Journal of Theoretical Biology, v. 253, p. 638–658, doi: 10.1016/j.jtbi.2008.03.032.

Li, S., Zhang, Y.-J., Sack, L., Scoffoni, C., Ishida, A., Chen, Y.-J., and Cao, K.-F., 2013, The heterogeneity and spatial patterning of structure and physiology across the leaf surface in giant leaves of *Alocasia macrorrhiza*: PLoS ONE, v. 8, e66016, doi: 10.1371/journal.pone.0066016.

Liang, J., Leng, Q., Höfig, D.F., Niu, G., Wang, L., Royer, D.L., Burke, K., Xiao, L., Zhang, Y., and Yang, H., 2022, Constraining conifer physiological parameters in leaf gas-exchange models for ancient CO_2 reconstruction: Global and Planetary Change, v. 209, article 103737, doi: 10.1016/j.gloplacha.2022.103737.

Maxbauer, D.P., Royer, D.L., and LePage, B.A., 2014, High Arctic forests during the middle Eocene supported by moderate levels of atmospheric CO_2: Geology, v. 42, p. 1027–1030, doi: 10.1130/g36014.1.

McElwain, J.C., 2018, Paleobotany and global change: important lessons for species to biomes from vegetation responses to past global change: Annual Review of Plant Biology, v. 69, p. 761–787, doi: 10.1146/annurev-arplant-042817-040405.

Nardini, A., Gortan, E., Ramani, M., and Salleo, S., 2008, Heterogeneity of gas exchange rates over the leaf surface in tobacco: an effect of hydraulic architecture?: Plant, Cell and Environment, v. 31, p. 804–812, doi: 10.1111/j.1365-3040.2008.01798.x.

Nguyen Tu, T.T., Bocherens, H., Mariotti, A., Baudin, F., Pons, D., Broutin, J., Derenne, S., and Largeau, C., 1999, Ecological distribution of Cenomanian terrestrial plants based on $^{13}C/^{12}C$ ratios: Palaeogeography, Palaeoclimatology, Palaeoecology, v. 145, p. 79–93, doi: 10.1016/S0031-0182(98)00092-3.

Nordt, L., Tubbs, J., and Dworkin, S., 2016, Stable carbon isotope record of terrestrial organic materials for the last 450 Ma yr: Earth-Science Reviews, v. 159, p. 103–117, doi: 10.1016/j.earscirev.2016.05.007.

Polissar, P.J., Rose, C., Uno, K.T., Phelps, S.R., and deMenocal, P., 2019, Synchronous rise of African C_4 ecosystems 10 million years ago in the absence of aridification: Nature Geoscience, v. 12, p. 657–660, doi: 10.1038/s41561-019-0399-2.

R Core Team, 2021, R: A language and environment for statistical computing: R Foundation for Statistical Computing, Vienna, Austria, https://www.R-project.org/.

Royer, D.L. and Hren, M.T., 2017, Carbon isotopic fractionation between whole leaves and cuticle: PALAIOS, v. 32, p. 199–205, doi: 10.2110/palo.2016.073.

Sack, L., Scoffoni, C., McKown, A.D., Frole, K., Rawls, M., Havran, J.C., Tran, H., and Tran, T., 2012, Developmentally based scaling of leaf venation architecture explains global ecological patterns: Nature Communications, v. 3, article 837, doi: 10.1038/ncomms1835.

Schlanser, K., Diefendorf, A.F., Greenwood, D.R., Mueller, K.E., West, C.K., Lowe, A.J., Basinger, J.F., Currano, E.D., Flynn, A.G., Fricke, H.C., Geng, J., Meyer, H.W., and Peppe, D.J., 2020, On geologic timescales, plant carbon isotope fractionation responds to precipitation similarly to modern plants and has a small negative correlation with pCO_2: Geochimica et Cosmochimica Acta, v. 270, p. 264–281, doi: 10.1016/j.gca.2019.11.023.

Schleser, G.H., 1990, Investigations of the $\delta^{13}C$ pattern in leaves of *Fagus sylvatica* L.: Journal of Experimental Botany, v. 41, p. 565–572, doi: 10.1093/jxb/41.5.565.

Spain, A. and Le Feuvre, R., 1997, Stable C and N isotope values of selected components of a tropical australian sugarcane ecosystem: Biology and Fertility of Soils, v. 24, p. 118–122, doi: 10.1007/BF01420231.

Spangenberg, J.E., Schweizer, M., and Zufferey, V., 2021, Carbon and nitrogen stable isotope variations in leaves of two grapevine cultivars (Chasselas and Pinot noir): implications for ecophysiological studies: Plant Physiology and Biochemistry, v. 163, p. 45–54, doi: 10.1016/j.plaphy.2021.03.048.

Received 18 January 2022; accepted 1 June 2022.